Supplementary Online Content

LeMaire SA, Zhang L, Luo W, et al. Effect of ciprofloxacin on susceptibility to aortic dissection and rupture in mice. *JAMA Surg*. Published online July 25, 2018. doi:10.1001/jamasurg.2018.1804

This supplementary material has been provided by the authors to give readers additional information about their work.

eMethods. Supplemental methods

Animal Studies

We evaluated the effects of ciprofloxacin on aortic aneurysm and dissection (AAD) development in a mouse model of moderate, sporadic AAD. Four-week-old wild-type (C57BL/6J) male and female mice were randomly assigned to the challenged or unchallenged group, aiming for an approximately 2:1 ratio. In the challenged group, mice were fed with a high-fat diet (HFD) containing 20% protein, 40% carbohydrate, 40% fat, and 1.25% cholesterol (Research Diets, Inc., D12108C, New Brunswick, NJ) for 8 weeks and were subcutaneously infused with 1000 ng/min/kg angiotensin II (AngII; Sigma-Aldrich Corp., St. Louis, MO) through an osmotic minipump (Model 2004; ALZA Scientific Products, Mountain View, CA) during the last 4 weeks. In the unchallenged control group, mice were fed a normal chow diet for 8 weeks and were infused with saline during the last 4 weeks. The challenged and unchallenged groups were further randomized and received either ciprofloxacin (100 mg/kg/day, 5% HCl in saline) or vehicle (5% HCl in saline) through daily gavage during the AngII or saline infusion period.

At the end of the 8-week study period, mice were euthanized with CO_2 inhalation. The aorta of each mouse was exposed and rinsed with cold phosphate-buffered saline (PBS). The peri-aortic tissues were removed. The aorta was excised and further cleaned and rinsed with cold PBS to remove any residual blood in the lumen. The aorta was then processed for AAD evaluation and tissue analysis. Different aortic segments were fixed in optimal cutting temperature (OCT) compound (Tissue-Tek; Miles Inc., Elkhart, Illinois) for immunofluorescence staining or were snap-frozen for protein analysis.

We chose the dose of ciprofloxacin based on the standard lower dose used to treat patients with common indications (500 mg/day, approximately 8.3 mg/kg/day) and used the standard conversion factor (12.3) for calculating an equivalent dose for mice.[1] We determined the sample size of mice based on preliminary data that indicated the overall incidence of AAD in all aortic segments was 40% for challenged mice that received vehicle and 85% for challenged mice that received ciprofloxacin. To show that the difference in the incidence of AAD between these groups was statistically significant (at α=0.05 with 80% power), we included 18 to 20 mice in each challenged group.

Measurement of Aortic Diameter

For each extracted aorta, we evaluated the ascending, arch, descending thoracic, suprarenal abdominal, and infrarenal aortic segments. Images of the aorta were obtained by using an Olympus SZX7 microscope at a magnification of 0.4X (scale bar=2 mm), and the diameter of each aortic segment was measured with DP2-BSW software (Olympus Corporation, Houston, TX). The median diameters of different aortic segments were compared between groups.

Evaluation of Aortic Aneurysm, Dissection, and Rupture

For each aortic segment, aortic dilatation was defined as an aortic diameter ≥1.25 times but <1.5 times the mean aortic diameter of the segment in unchallenged mice treated with vehicle. Aortic aneurysm was defined as an aortic diameter ≥1.5 times the mean aortic diameter of the segment in unchallenged mice treated with vehicle. Aortic dissection was defined as the presence of hematoma within the aortic wall detected on gross examination, or as the presence of layer separation within the aortic media or medial-adventitial boundary (with a false lumen hematoma) detected on aortic histology. Aortic rupture and premature death were documented.

Classification of AAD Severity

The severity of AAD was classified as one of the following by using our previously reported[2] modification of the classification system described by Daugherty and colleagues[3]: normal aorta; dilated aorta; aortic aneurysm without dissection; aortic dissection (as indicated by intramural

thrombus) without aneurysm; aortic aneurysm with dissection; or ruptured aorta. We defined the category *AAD* as the presence of aneurysm, dissection, or rupture. *Severe AAD* was defined as the presence of dissection or rupture. Aneurysmal tissue was evaluated by 4 independent observers who were blinded to the experimental groups. In the case of a discrepancy, the observers discussed the case and agreed on the classification.

Elastic Fiber Staining

Aortic sections were stained with Verhoeff–Van Gieson elastin staining by using the Elastic Stain Kit (Sigma-Aldrich) according to the manufacturer's instructions. Aortic sections were examined by 2 independent observers who were blinded to the experimental groups. Elastic fiber fragmentation was scored (Grade 0 = none; Grade 1 = minimal; Grade 2 = moderate; Grade 3 = severe).

Immunofluorescence Staining

OCT-embedded aortic sections and treated cells were fixed with Cytofix (BD Biosciences, San Jose, CA) on slides and permeabilized with Perm/Wash (BD Biosciences). Nonspecific staining was reduced by blocking with 5% normal blocking serum. The sections or cells were then incubated with primary antibody at room temperature for 2 hours or at 4°C overnight, washed with PBS, and incubated with secondary antibody conjugated to an Alexa Fluor dye such as Alexa Fluor-488, -555, or -647 (ThermoFisher Scientific, Waltham, MA). Nuclei were counterstained with 4',6-diamidino-2-phenylindole (DAPI). Slides incubated with secondary antibody alone were used as negative controls. Primary and secondary antibodies used for immunofluorescence staining are listed in eTable.

Tissue sections were examined by using a Leica microscope (Leica Microsystems Inc., Buffalo Grove, IL) and by using a Leica SP5 confocal microscope (Leica). For quantification, images were captured from 3 to 4 randomly selected visual fields (excluding the thrombosed false lumen) per aortic section (magnification, 200X). The positive-staining area and the evaluated aortic area were measured by using Image-Pro Plus V7.0 software (Media Cybernetics, Inc., Bethesda, MD), and the positive-staining area was normalized to the evaluated aortic area. The same exposure time was used for all samples. Aortic tissues from 5 mice in each group were analyzed. The mean or median positive percentages were calculated and compared between groups.

MMP Activity Determined by Using In Situ Zymography

MMP activity in the aortic wall was determined by using gelatin conjugated with quenched fluorescein (DQ gelatin; Invitrogen Corporation, Carlsbad, CA) as a substrate, according to the manufacturer's instructions. Briefly, frozen aortic sections were incubated with 0.1 mg/mL DQ gelatin in 1% low-melting agarose at 37°C for 48 hours. Fluorescence was examined by using fluorescence microscopy. Zymographic images were acquired by using identical setting and exposure times.

Terminal Deoxynucleotidyl Transferase dUTP Nick End Labeling (TUNEL) Assay

Frozen sections of aorta or treated SMCs were fixed with 4% paraformaldehyde in PBS for 10 minutes and permeabilized with 0.2% Triton X-100 for 5 minutes. The fixed tissues or cells were incubated for 1 hour at 37°C with TUNEL reaction mixture containing terminal deoxynucleotidyl transferase. After TUNEL staining, nuclei were counterstained with DAPI (0.1 g/mL). Terminal deoxynucleotidyl transferase–free labeling mixture was used in negative control reactions. For each aortic section or cell treatment condition, we captured images from 5 randomly selected views. For each image, the number of positive cells and the number of total nuclei were quantified, and the percentage of positive cells was calculated.

Cell Culture and Gene Silencing
Male human aortic smooth muscle cells (SMCs; Invitrogen) were cultured in smooth muscle media (Invitrogen) with 10% fetal bovine serum. Cells passaged fewer than 8 times were used in experiments. SMCs were treated with 0 to 200 μg/ml ciprofloxacin for 24 hours. In some experiments, SMCs were first transfected with 50 or 100 nM of cGAS siRNA, STING siRNA, or IRF3 siRNA (Invitrogen) by using Lipofectamine (Invitrogen) according to the manufacturer's instructions. Transfected cells were then treated with 100 μg/ml ciprofloxacin for 24 hours. Transfection efficiency was confirmed with western blot analysis.

LOX Activity Assay
LOX activity was measured by using a Lysyl Oxidase Activity Assay Kit (Fluorometric) (Abcam, ab112139), which contains LOX substrate. Upon transformation by LOX, the substrate releases hydrogen peroxide and fluoresces red through HRP-coupled reactions. The assay was performed according to the manufacturer's instructions. Briefly, cell culture media was collected and incubated with LOX substrate at 37°C for 30 minutes in the dark. The fluorescence signal was detected at excitation/emission wavelengths of 540/590 nm by using a Tecan Infinite M200 PRO Multi-Detection Microplate Reader.

Western Blot Analysis
Protein levels were determined in lysates from treated cells as previously described.[2] Protein samples (15 μg per lane) were subjected to sodium dodecyl sulfate (SDS) polyacrylamide gel electrophoresis by using Mini-TGX gels (4-20%; Bio-Rad Laboratories, Inc., Hercules, CA) and were transferred to PVDF membrane by using Bio-Rad Turbo transfer. The membranes were blocked, incubated with primary antibody, washed, and incubated with horseradish peroxidase (HRP)-conjugated anti-rabbit or anti-mouse secondary antibody. All primary and secondary antibodies used for western blotting are listed in eTable. Protein bands were visualized by using Clarity Enhanced Chemiluminescence (Bio-Rad) and were exposed with HyBlot ES autoradiography film (Denville Scientific Inc., Holliston, MA). The blots were quantified with densitometry by using the Quantity One imaging program (Bio-Rad). Protein levels were normalized to those of β-actin or GAPDH and were expressed as the percentage of the no-treatment control.

Quantitative Real-Time Polymerase Chain Reaction (qRT-PCR)
Total RNA from treated cells was extracted with Trizol (Invitrogen) according to the manufacturer's protocol. The mRNA was reverse-transcribed with the iScript cDNA synthesis kit (Bio-Rad). qRT-PCR was performed with the iCycler iQ Real-Time PCR detection system (Bio-Rad). Primers were designed with Beacon Designer 2.0 software (Premier Biosoft International, Palo Alto, CA). We used the following primers for human *LOX*: forward 5'-CGGCGGAGGAAAACTGTCT -3' and reverse 5'- TCGGCTGGGTAAGAAATCTGA -3'. mRNA levels were determined by normalizing the cycle threshold (Ct) of *LOX* to the Ct of β-actin. The relative levels of mRNA were expressed as the percentage of the no-treatment control and were compared among groups.

MMP Activity Determined by Using In Gel Zymography
Aortic SMC culture supernatants and cell lysates were harvested. Samples (10 μL each) were di-luted in Novex Tris-Glycine Sodium Dodecyl Sulfate Sample Buffer (Thermofisher), loaded on Novex 10% Zymogram Plus Protein Gels (Gelatin), and electrophoresed at 125 V for 2 hours. Gels were renatured in Zymogram Renaturing Buffer (Thermofisher) at room temperature for 30 minutes and were developed in Zymogram Developing Buffer (Thermofisher) at 37°C overnight. Gels were stained with Coomassie staining solution (0.1% Coomassie R250 in 40% ethanol and

10% acetic acid) for 2 hours and destained in destaining solution (10% ethanol and 7.5% acetic acid). Images of stained gels were captured by using a CanoScan 9950F Flatbed Scanner.

Cell Proliferation Analysis by Using the EdU Assay

SMC proliferation was analyzed by measuring DNA synthesis with the Click-iT EdU Alexa Fluor 488 Flow Cytometry Assay Kit (Life Technologies, Carlsbad, CA). Briefly, cells were incubated with 10 μM EdU (5-ethynyl-2′-deoxyuridine) at 37°C for 2 hours. Cells were then harvested, fixed in Click-iT fixative agent for 15 min, and permeabilized in Click-iT saponin-based permeabilization reagent for 15 minutes. Cells were then incubated with Click-iT reaction cocktails for 30 minutes in the dark. EdU incorporation was also observed by using immunofluorescence microscopy (Olympus,Tokyo, Japan). Images were acquired and analyzed with ImageJ software (NIH, Bethesda, MD). Fluorescence signals were detected by using an FC500 flow cytometer (Beckman Coulter Inc., Indianapolis, IN), and the data were analyzed by using MultiCycle software (Phoenix Flow Systems, San Diego, CA).

Analysis of Cell Death by Using Annexin V/Propidium Iodide (PI) Staining

Cell death was detected by performing flow cytometry analysis of annexin V (apoptotic cell marker) and propidium iodide (PI) (necrotic cell marker) by using an annexin V-FITC/PI staining kit (11858777001, Roche). Treated cells were harvested, washed with PBS, and stained with annexin V-FITC and PI in the dark at room temperature for 15 minutes. Samples were immediately analyzed by using a flow cytometer (BD Biosciences), and the data were analyzed by using BD FACSDiva software (BD Biosciences).

Detection of Cytosolic DNA (Mitochondrial and Nuclear) by Using PCR

Treated aortic SMCs were lysed in cell lysis buffer (ThermoFisher Scientific) and centrifuged at 700 × g for 10 minutes at 4°C to remove the nuclei and intact cells. The volume of the supernatant was normalized according to the protein concentration. The cell lysate was further centrifuged at 10,000 × g for 30 minutes at 4°C to isolate the cytosolic fraction, from which DNA was precipitated and isolated.

Mitochondrial DNA (mtDNA) was detected with quantitative PCR by using coding sequences of mitochondrial cytochrome c oxidase 1 (mtCOI) as primer sequences. Nuclear DNA was measured with PCR by using coding sequences of 18S ribosomal RNA (18S rDNA) as primer sequences. The primers for human mtCOI were as follows: forward 5'-GCC CCC GAT ATG GCG TTT-3' and reverse 5'-GTT CAA CCT GTT CCT GCT CC-3'. The primers for human 18S rDNA were forward 5'-TAG AGG GAC AAG TGG CGT TC-3' and reverse 5'-CGC TGA GCC AGT CAG TGT-3'.

Detection of Cytosolic DNA by Using Immunofluorescence Staining

Treated SMCs were incubated with MitoTracker (ThermoFisher Scientific) at 37°C for 30 minutes. Cells were then fixed and permeabilized with BD Cytofix/Cytoperm solution (BD Biosciences), blocked with 10% donkey serum, incubated with anti-dsDNA antibody (Abcam, ab27156, 1:1000) to detect double-stranded DNA (dsDNA), and incubated with fluorescently labeled secondary antibody (Invitrogen, A28175,1:500). Slides were mounted and observed with a Leica SP5 confocal microscope (Leica). Images were captured and analyzed by using LAS AF Lite software (Leica). The ratios of mtDNA copy number to nuclear DNA copy number were compared between groups.

Mitochondrial Transmembrane Potential Analysis

Mitochondrial transmembrane potential (Δψ) was measured by using the fluorescent probe JC-1 (5, 5′, 6, 6′-tetrachloro-1, 1′, 3, 3′-tetraethylbenzimidazol carbocyanine iodide), a cationic fluorescent dye that forms red aggregates in polarized functional mitochondria while remaining

as a green monomer outside depolarized dysfunctional mitochondria. Cells were incubated with 20 μM JC-1 at 37°C for 20 minutes and washed twice with PBS. Cells were observed with a Leica SP5 confocal microscope (Leica). The red and green fluorescence signals were measured, and the red/green fluorescence ratio was calculated and compared among groups.

Statistical Analysis

Data were analyzed by using SPSS software, version 22.0 (SPSS Inc., Chicago, IL). Categorical variables were compared between groups by using the chi squared test. All quantitative data are presented as the mean ± standard deviation. Normality of the data was examined by using the Kolmogorov-Smirnov test. For variables without violation of the normality assumption, two-group comparisons were performed by using the t test. Multi-group comparisons were performed by using one-way analysis of variance for data with unequal variances. For variables with violation of the normality assumption, two-group comparisons were performed by using the Mann-Whitney test, and multi-group comparisons were performed by using the Kruskal-Wallis test. Kaplan-Meier survival curves were plotted to analyze survival rates in mice; curves were compared by using the log-rank test. For all statistical analyses, two-tailed probability values were used. A probability value (P) of $P<0.05$ was considered significant.

eTable. Antibodies used for western blot and immunostaining experiments

Antibody	Vendor	Catalog number	Dilution
Western blot analysis			
Anti-LOX antibody	Abcam	ab-31238	1:1000
Anti-Fibrillin-1	Santa Cruz	sc-20084	1:250 (BSA)
Anti-Collagen I	Abcam	ab-34710	1:1000
Anti-Collagen III	Abcam	ab-7778	1:1000
Anti-MMP-1 (3B6)	Santa Cruz	sc-21731	1:250 (BSA)
Anti-MMP-2	Abcam	ab-37150	1:1000
Anti-MMP-9	Santa Cruz	sc-6841	1:250 (BSA)
Anti-MMP-9 (E-11)	Santa Cruz	sc-393859	1:250 (BSA)
Anti-TIMP-1	Santa Cruz	sc-21734	1:250 (BSA)
Anti-TIMP-1 (H-150)	Santa Cruz	sc-5538	1:250 (BSA)
Anti-RIP3	Santa Cruz	sc-374639	1:250 (BSA)
Anti-MLKL	Millipore	cs-214789	1:1000
Anti-cGAS Antibody	EMD Millipore	abf-124	1:2000
Anti-STING (D2P2F)	Cell Signaling	13647	1:1000
Anti-IRF-3 (D6I4C) XP®	Cell Signaling	11904	1:1000
Anti-IRF-3	Cell Signaling	4302	1:1000
Anti-phosph-IRF3 (Ser396)	Cell Signaling	4947	1:500
Anti-NAK/TBK1[EP611Y]	Abcam	ab-40676	1:1500
Goat anti-rabbit IgG-HRP	Santa Cruz	sc-2004	1:5000
Goat anti-mouse IgG-HRP	Santa Cruz	sc-2005	1:5000
Immunostaining			
Anti-dsDNA antibody	Abcam	ab-27156	1:1000
Anti-SM22	Abcam	ab-10135	1:300
Anti-LOX antibody	Abcam	ab-31238	1:1000
Anti-Collagen I	Abcam	ab-34710	1:1000
Anti-Collagen III	Abcam	ab-7778	1:1000
Anti-MMP-1 (3B6)	Santa Cruz	sc-21731	1:250 (BSA)
Anti-MMP-9 (E-11)	Santa Cruz	sc-393859	1:250 (BSA)
Anti-TIMP-1	Santa Cruz	sc-21734	1:250
Anti-TIMP-1 (H-150)	Santa Cruz	sc-5538	1:250
Anti-RIP3	Santa Cruz	sc-374639	1:250
Anti-MLKL	Millipore	cs-214789	1:200

BSA indicates bovine serum albumin.

eFigure 1. Increased aortic destruction, decreased LOX protein expression, increased MMP activity, and increased reactive oxygen species production in the aortic wall of challenged mice that received ciprofloxacin

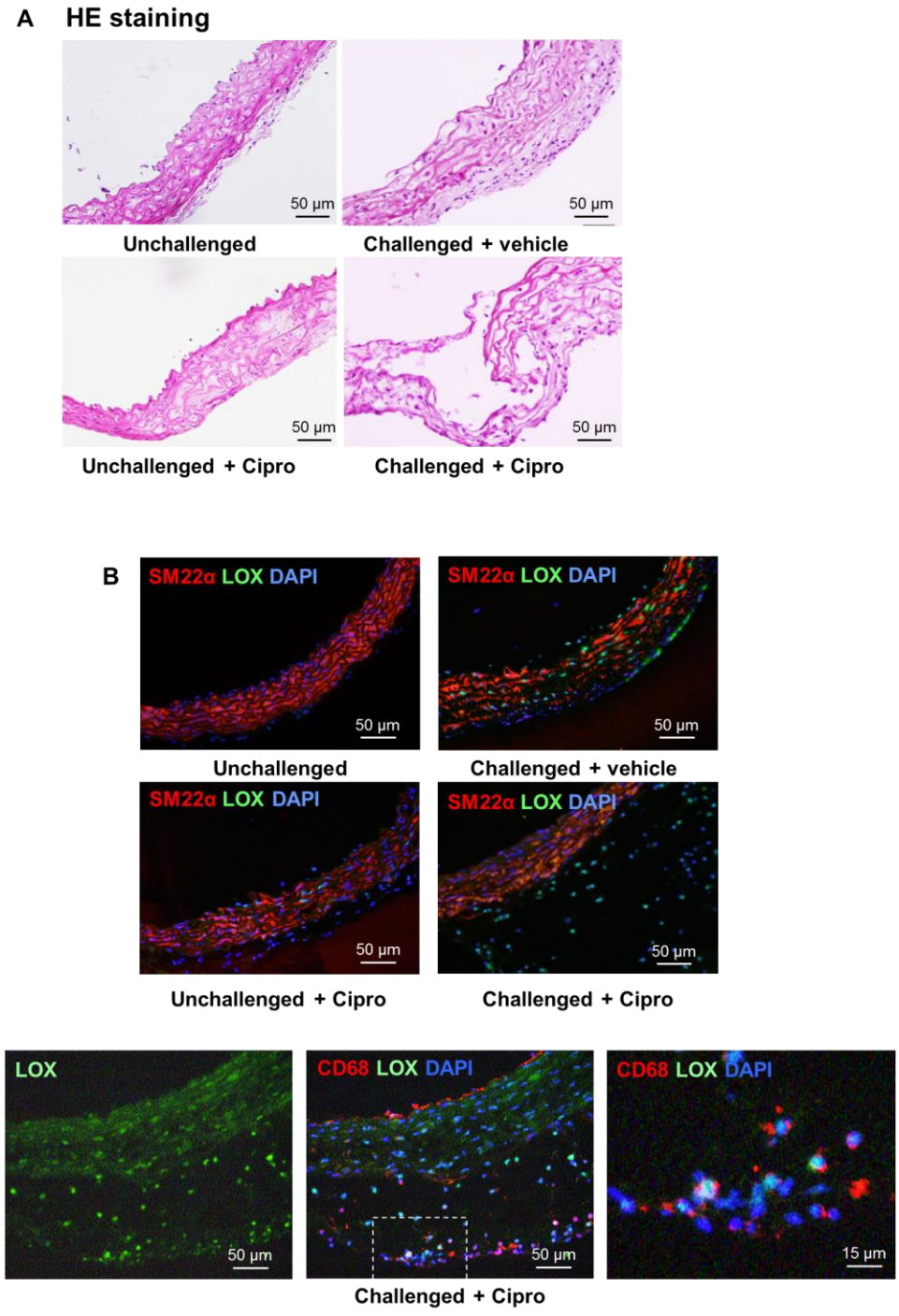

C **MMP activity (*in situ* Zymography)**

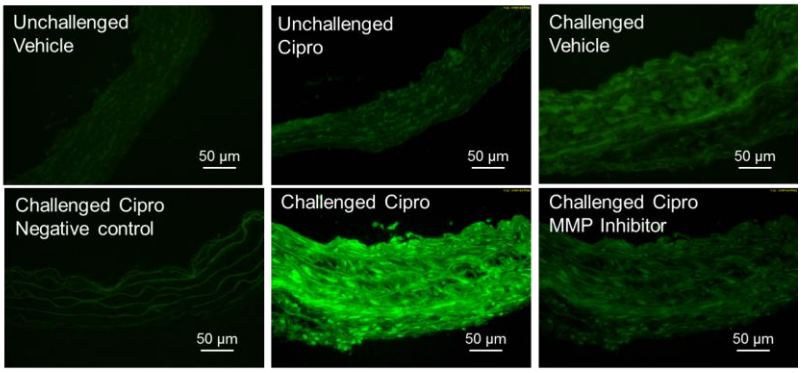

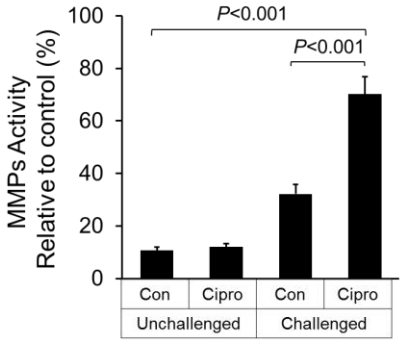

D

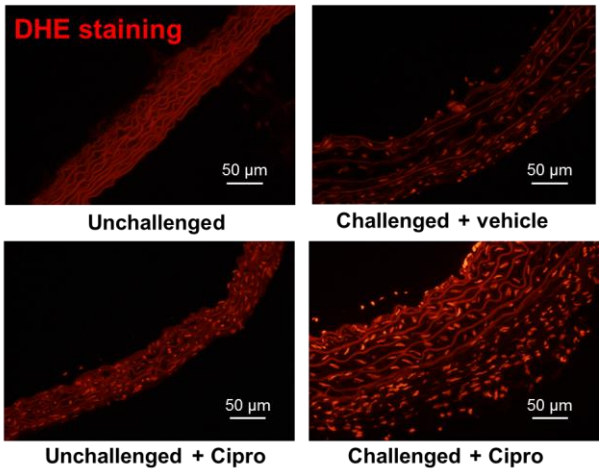

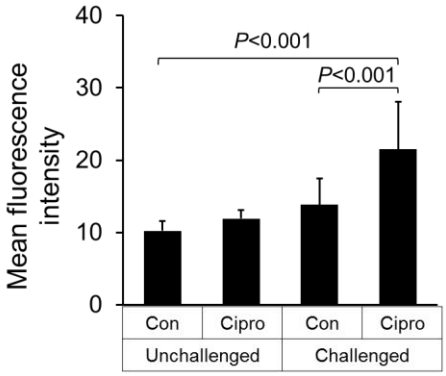

A, Representative images of hematoxylin and eosin (HE) staining showing aortic dissection in the aortic wall of challenged mice that received ciprofloxacin. B, Representative images of immunofluorescence staining showing that the challenged-induced expression of LOX in the aortic wall of mice that received vehicle was compromised in mice that received ciprofloxacin, especially in the medial layer. Representative images of double staining showing LOX expression in smooth muscle cells (SMCs) in the media and in macrophages in the adventitia. C, Representative zymography images showing increased MMP activity in aortas from challenged mice that received ciprofloxacin. Aortic tissues from 5 mice in each group were analyzed. For the above quantification, the positive-staining area from 3 to 4 randomly selected microscopic fields (magnification, 200X) per tissue section was measured and normalized with the evaluated aortic area. The comparison of mean positive-staining values among groups is shown. D, Representative images of dihydroethidium (DHE) staining and quantification (mean positive-staining area normalized to the evaluated aortic area) showing increased reactive oxygen species (ROS) production in the aortic wall of challenged mice that received ciprofloxacin.

eFigure 2. Downregulation of extracellular matrix proteins and upregulation of MMP expression and activity in cultured aortic smooth muscle cells (SMCs) treated with ciprofloxacin

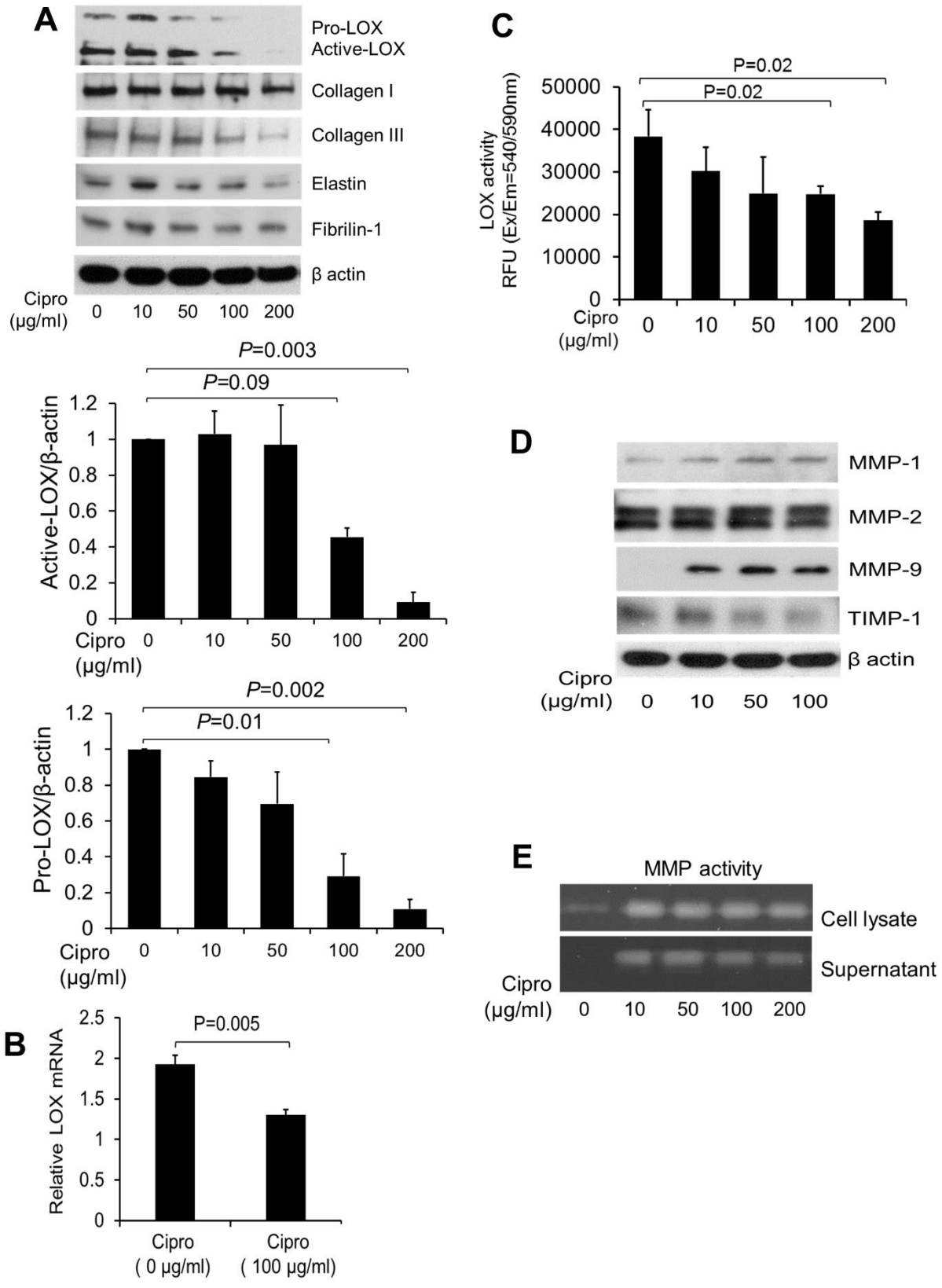

Aortic SMCs were treated with ciprofloxacin (0-200 μg/ml) for 24 hours (3-5 biologic replicates). A, Representative western blot analysis and quantification showing that ciprofloxacin treatment decreased levels of LOX (both pro and active forms) in a dose-dependent manner (3-5 biologic replicates). B, Real-time PCR results showing that ciprofloxacin treatment decreased *LOX* mRNA levels (3 biologic replicates). C, LOX activity assay results showing that ciprofloxacin treatment decreased LOX activity in a dose-dependent manner (3 biologic replicates). D, Representative western blot analysis showing that ciprofloxacin treatment decreased TIMP-1 but increased MMP-1 and MMP-9 levels (3-5 biologic replicates). E, Representative results of zymography analysis showing that ciprofloxacin treatment increased MMP activity (3 biologic replicates).

eFigure 3. Inhibition of cell proliferation and induction of cell injury in cultured aortic SMCs treated with ciprofloxacin

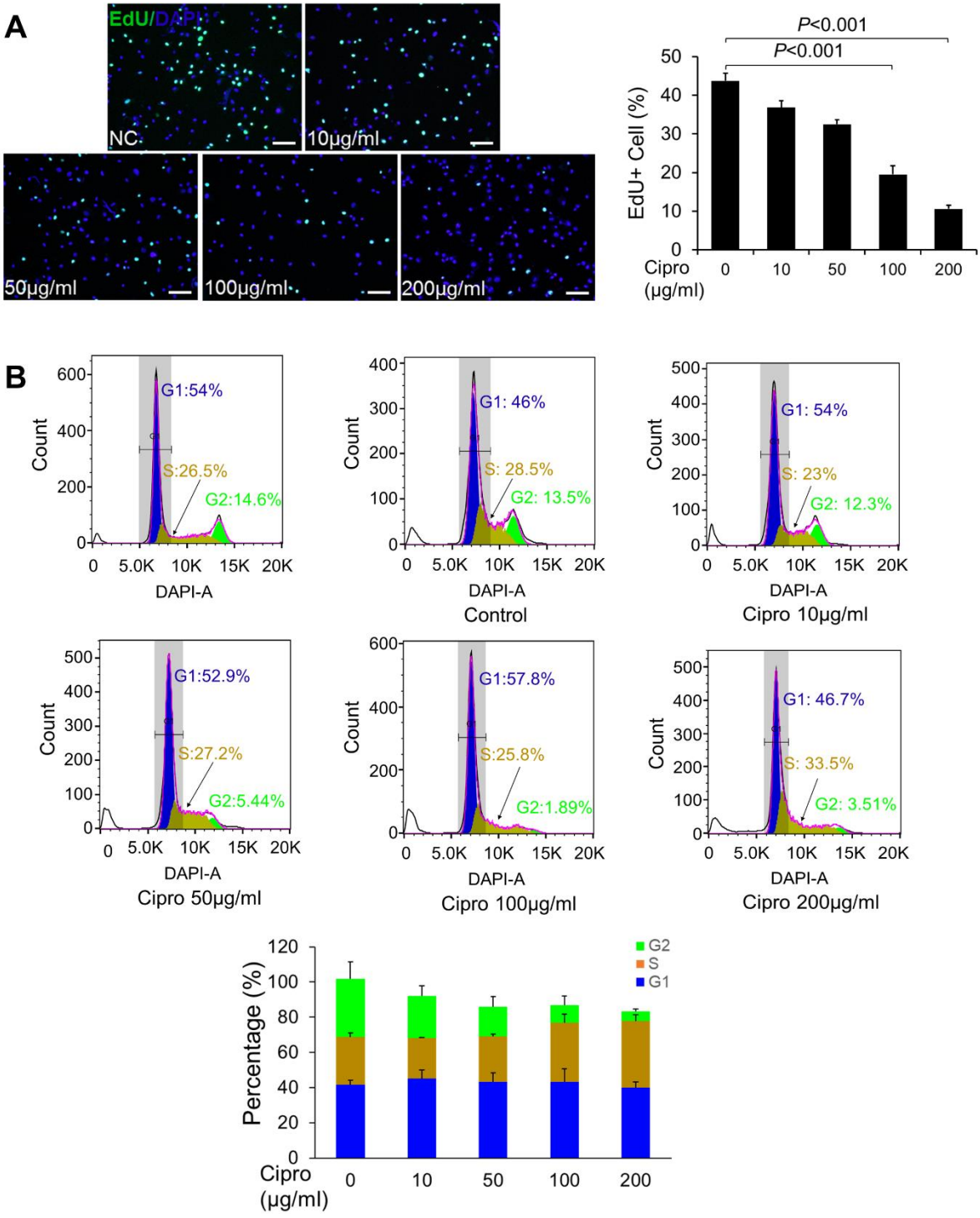

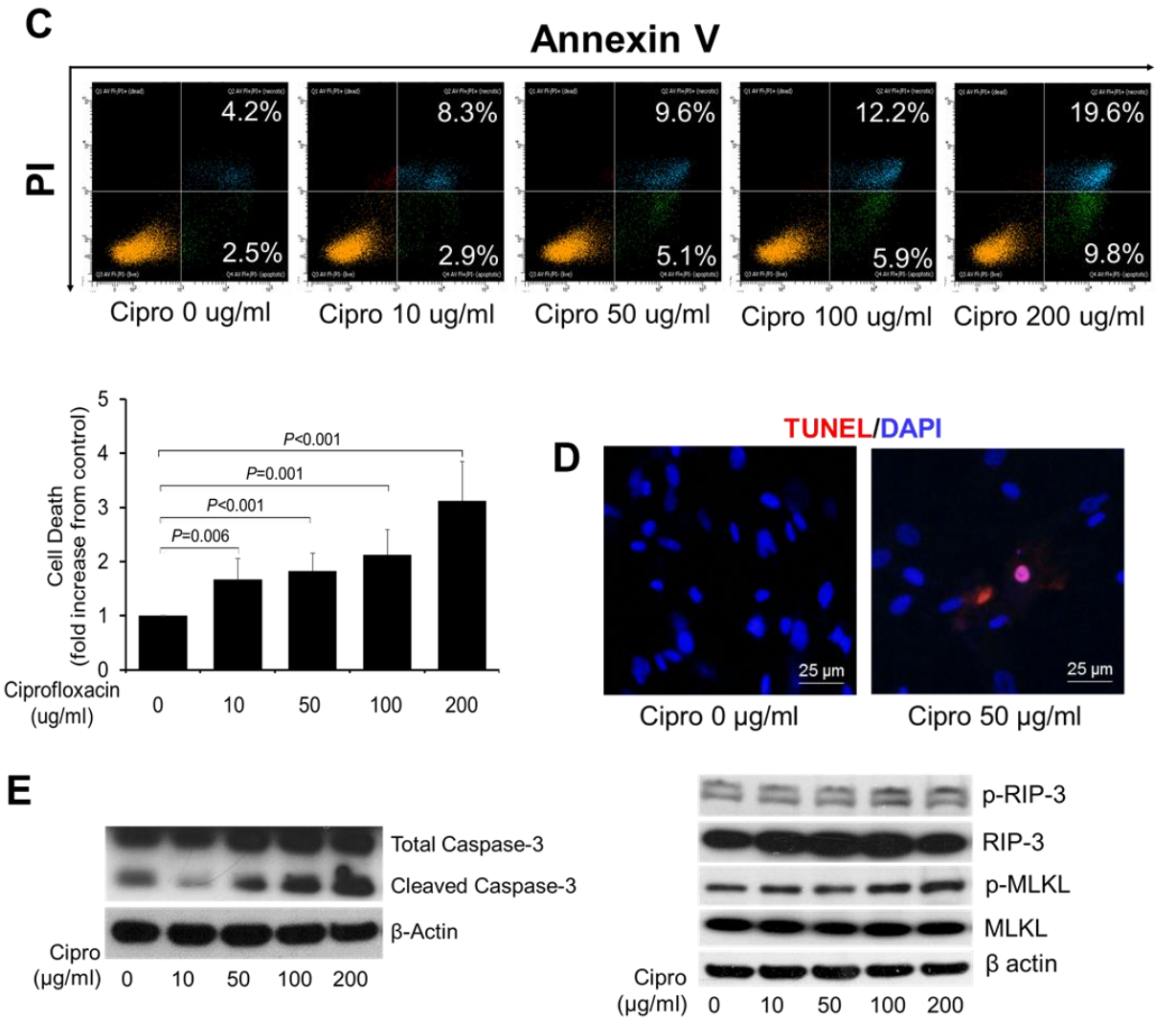

Aortic SMCs were treated with ciprofloxacin (0-200 μg/ml) for 24 hours (3-5 biologic replicates). A, Representative immunofluorescence and flow cytometry analysis of EdU (5-ethynyl-2′-deoxyuridine) staining showing that ciprofloxacin inhibited cell proliferation in a dose-dependent manner (3 biologic replicates). B, Cell cycle distribution of SMCs measured by flow cytometric analysis showing that ciprofloxacin inhibited cell G2 phase in a dose-dependent manner (3 biologic replicates). C, Representative flow cytometry analysis of propidium iodide (PI) and annexin V staining showing that ciprofloxacin induced cell death in a dose-dependent manner (5 biologic replicates). D, Representative results of terminal deoxynucleotidyl transferase dUTP nick end labeling (TUNEL) analysis showing that ciprofloxacin increased the number of TUNEL-positive cells (3 biologic replicates). E, Representative western blot analysis showing that ciprofloxacin treatment increased caspase-3 cleavage (i.e., activation) in a dose-dependent manner and the phosphorylation of MLKL (3 biologic replicates).

eFigure 4. Increased DNA damage and its release into the cytosol and the activation of cytosolic DNA sensor signaling in aortic SMCs treated with ciprofloxacin

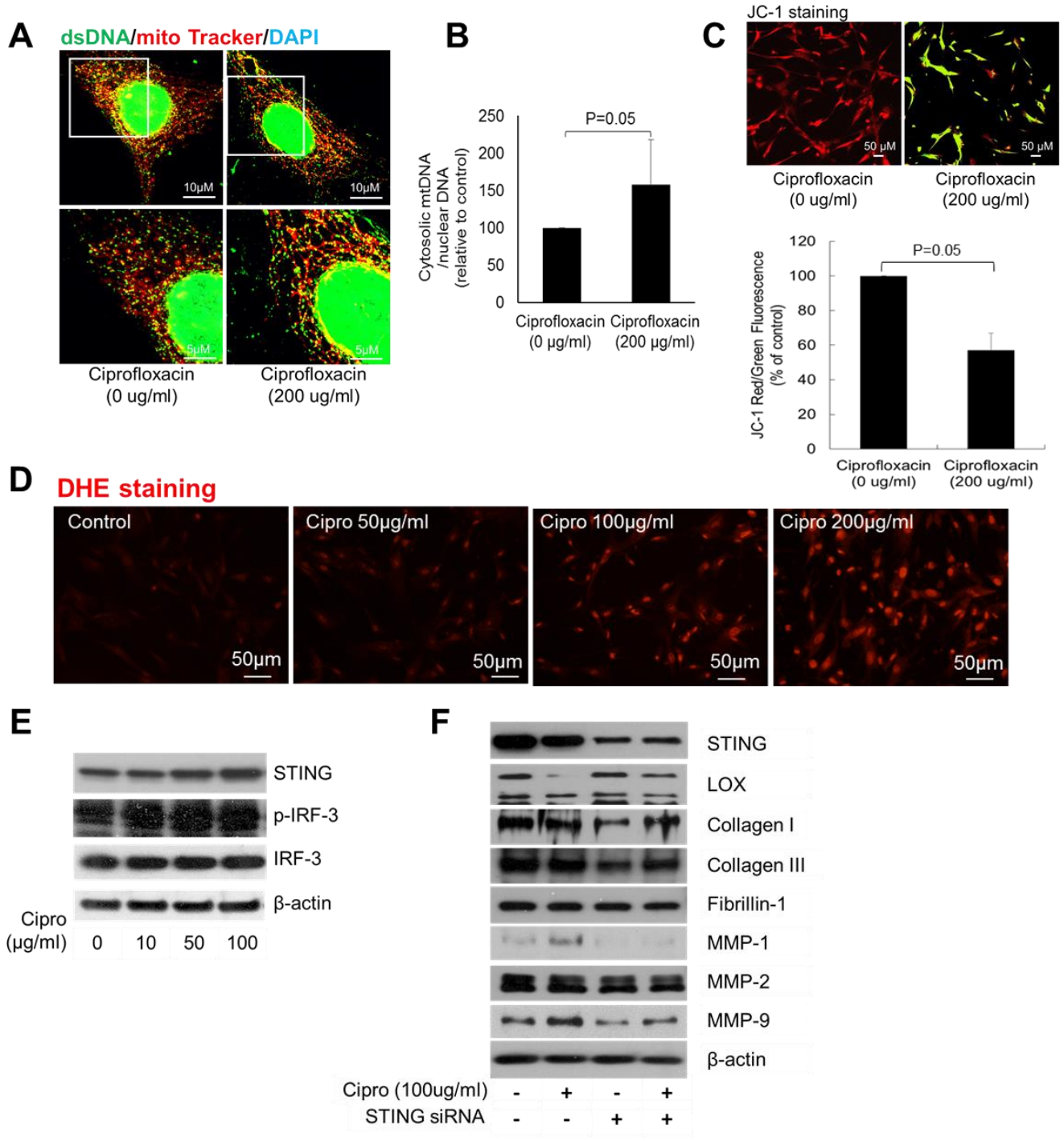

A-D, Aortic SMCs were treated with the indicated dose of ciprofloxacin for 24 hours (n=3-4 biologic replicates). A, Costaining of double-stranded DNA (dsDNA) with anti-dsDNA antibody and mitochondria with MitoTracker showing the detection of nuclear DNA (dsDNA in the nucleus), mitochondrial DNA (mtDNA, dsDNA that colocalized with MitoTracker), and cytosolic DNA (dsDNA that did not colocalize with either mitochondria or the nucleus). Ciprofloxacin triggered the release of dsDNA into the cytosol. B, Cytosolic nuclear DNA and mitochondrial DNA were measured by performing PCR analysis of DNA in the cytosolic fraction by using nuclear or mitochondrial DNA sequences as primer sequences. Ciprofloxacin increased the ratio of mtDNA/nuclear DNA (n=3 biologic replicates). C, JC-1 staining showing that ciprofloxacin decreased the number of red aggregates and increased the number of green monomers (thus decreasing the red/green fluorescence ratio), indicating reduced mitochondrial membrane potential ($\Delta\psi_m$) and mitochondrial dysfunction. D, Representative dihydroethidium (DHE) staining showing that ciprofloxacin treatment increased reactive oxygen species (ROS) production. E, Representative western blot analysis showing that ciprofloxacin increased the expression of STING and the phosphorylation of IRF3 in aortic SMCs (n=3 biologic replicates). F, Representative western blot analysis showing the effect of silencing STING on the ciprofloxacin-induced dysregulation of LOX and MMP expression. Aortic SMCs were transfected with scramble siRNA or STING siRNA and then treated with or without 100 µg/ml of ciprofloxacin for 24 hours (n=3-5 biologic replicates). Silencing the expression of STING prevented ciprofloxacin-induced dysregulation of LOX and MMP expression.

eAppendix 1. DNA damage and release to the cytosol, mitochondrial dysfunction, and activation of cytosolic DNA sensor signaling by ciprofloxacin

We next investigated the mechanisms by which ciprofloxacin dysregulates aortic SMC gene expression and induces cell injury. Quinolones such as ciprofloxacin are known to target DNA topoisomerases,[4-13] which are enzymes that generate a transient DNA double-strand break, untangle duplex DNA, and release torsional DNA stress to allow for DNA replication.[14,15] Because stabilized DNA-topoisomerase complexes induced by ciprofloxacin can generate DNA double-strand breaks,[16-18] we examined whether ciprofloxacin causes DNA damage and the release of DNA into the cytosol in aortic SMCs. By costaining dsDNA and mitochondria (MitoTracker), we detected cytosolic DNA—dsDNA that did not colocalize with either mitochondria or nuclei (eFigure 4A). We found that cytosolic DNA was barely detectable in untreated SMCs but was markedly increased in SMCs treated with ciprofloxacin. Furthermore, when we performed PCR analysis of cytosolic DNA by using mitochondrial DNA or nuclear DNA sequences as primers, we found that ciprofloxacin significantly increased the amount of nuclear DNA (data not shown) and mitochondrial DNA in the cytosolic fraction, as well as the ratio of mitochondrial DNA/nuclear DNA (eFigure 4B). These data suggest that ciprofloxacin causes nuclear and mitochondrial DNA damage and the release of DNA into the cytosol.

Because DNA topoisomerases are also present in mitochondria, ciprofloxacin may target mitochondrial DNA topoisomerases and cause mitochondrial DNA damage, which is known to cause DNA depletion and mitochondrial dysfunction.[13,19-23] We therefore examined the effects of ciprofloxacin on mitochondrial function by measuring mitochondrial membrane potential ($\Delta\psi_m$) in aortic SMCs by using JC-1 staining. JC-1 is a cationic fluorescent dye that forms red aggregates in polarized functional mitochondria while remaining as a green monomer outside depolarized mitochondria. In aortic SMCs, ciprofloxacin treatment decreased the number of red aggregates and increased the number of green monomers, resulting in a decreased red/green fluorescence ratio (eFigure 4C) that indicated a reduced $\Delta\psi_m$ and mitochondrial dysfunction. Consistent with this finding, we observed a significant increase in intracellular ROS in ciprofloxacin-treated aortic SMCs (eFigure 4D).

Finally, we examined the mechanism underlying DNA damage–induced ECM gene dysregulation in ciprofloxacin-treated aortic SMCs. Recent studies have suggested that the STING (stimulator of interferon genes) pathway is an important signaling pathway that detects cytosolic DNA and triggers the inflammatory response.[24-28] Therefore, we investigated whether this mechanism is activated by ciprofloxacin treatment and mediates ciprofloxacin-induced ECM gene dysregulation in aortic SMCs. We found that ciprofloxacin treatment increased the expression of STING and the phosphorylation of IRF3 (eFigure 4E), indicating the activation of this pathway. Importantly, silencing STING with siRNA partially prevented the ciprofloxacin-induced decrease in LOX and increase in MMP-1 and MMP-9 protein expression (eFigure 4F), suggesting that STING is involved in the ciprofloxacin-induced suppression of LOX expression and the induction of MMP expression. Together, these data suggest that ciprofloxacin treatment promotes the release of nuclear and mitochondrial DNA into the cytosol and the activation of the cytosolic DNA sensor STING, which may mediate the effect of ciprofloxacin on the disruption of ECM integrity.

eAppendix 2. Two independent observational clinical studies suggesting that fluoroquinolone use may be associated with an increased risk of aortic aneurysm and dissection

In a case-control analysis of 1477 patients and 147,700 matched controls in Taiwan, Lee and colleagues[29] found that fluoroquinolone use was associated with an increased risk of aortic aneurysm or dissection (rate ratio, 2.43; 95% confidence interval [CI], 1.83-3.22). In a population-based longitudinal cohort study of 1,744,360 individuals ≥ 65 years of age in Ontario, Canada, Daneman and colleagues[30] found that aortic aneurysms were more common in patients treated with fluoroquinolones, especially in those who were currently receiving treatment (hazard ratio [HR], 2.24; 95% CI, 2.02-2.49).

eReferences

1. Nair AB, Jacob S. A simple practice guide for dose conversion between animals and human. *J Basic Clin Pharm.* 2016;7(2):27-31.
2. Wu D, Ren P, Zheng Y, et al. NLRP3 (nucleotide oligomerization domain-like receptor family, pyrin domain containing 3)-Caspase-1 inflammasome degrades contractile proteins: implications for aortic biomechanical dysfunction and aneurysm and dissection formation. *Arterioscler Thromb Vasc Biol.* 2017.
3. Daugherty A, Manning MW, Cassis LA. Angiotensin II promotes atherosclerotic lesions and aneurysms in apolipoprotein E-deficient mice. *J Clin Invest.* 2000;105(11):1605-1612.
4. Hussy P, Maass G, Tummler B, Grosse F, Schomburg U. Effect of 4-quinolones and novobiocin on calf thymus DNA polymerase alpha primase complex, topoisomerases I and II, and growth of mammalian lymphoblasts. *Antimicrob Agents Chemother.* 1986;29(6):1073-1078.
5. Oomori Y, Yasue T, Aoyama H, Hirai K, Suzue S, Yokota T. Effects of fleroxacin on HeLa cell functions and topoisomerase II. *J Antimicrob Chemother.* 1988;22 Suppl D:91-97.
6. Pessina A, Neri MG, Muschiato A, Mineo E, Cocuzza G. Effect of fluoroquinolones on the in-vitro proliferation of myeloid precursor cells. *J Antimicrob Chemother.* 1989;24(2):203-208.
7. Bredberg A, Brant M, Jaszyk M. Ciprofloxacin-induced inhibition of topoisomerase II in human lymphoblastoid cells. *Antimicrob Agents Chemother.* 1991;35(3):448-450.
8. Elsea SH, McGuirk PR, Gootz TD, Moynihan M, Osheroff N. Drug features that contribute to the activity of quinolones against mammalian topoisomerase II and cultured cells: correlation between enhancement of enzyme-mediated DNA cleavage in vitro and cytotoxic potential. *Antimicrob Agents Chemother.* 1993;37(10):2179-2186.
9. Perrone CE, Takahashi KC, Williams GM. Inhibition of human topoisomerase IIalpha by fluoroquinolones and ultraviolet A irradiation. *Toxicol Sci.* 2002;69(1):16-22.
10. Bromberg KD, Burgin AB, Osheroff N. Quinolone action against human topoisomerase IIalpha: stimulation of enzyme-mediated double-stranded DNA cleavage. *Biochemistry (Mosc).* 2003;42(12):3393-3398.
11. Kloskowski T, Gurtowska N, Olkowska J, et al. Ciprofloxacin is a potential topoisomerase II inhibitor for the treatment of NSCLC. *Int J Oncol.* 2012;41(6):1943-1949.
12. Bisacchi GS, Hale MR. A "double-edged" scaffold: antitumor power within the antibacterial quinolone. *Curr Med Chem.* 2016;23(6):520-577.
13. Fu Y, Yang Y, Zhou S, et al. Ciprofloxacin containing Mannich base and its copper complex induce antitumor activity via different mechanism of action. *Int J Oncol.* 2014;45(5):2092-2100.
14. Wang JC. DNA topoisomerases. *Annu Rev Biochem.* 1996;65:635-692.
15. Pommier Y, Leo E, Zhang H, Marchand C. DNA topoisomerases and their poisoning by anticancer and antibacterial drugs. *Chem Biol.* 2010;17(5):421-433.
16. Drlica K, Zhao X. DNA gyrase, topoisomerase IV, and the 4-quinolones. *Microbiol Mol Biol Rev.* 1997;61(3):377-392.
17. Hooper DC. Mechanisms of action and resistance of older and newer fluoroquinolones. *Clin Infect Dis.* 2000;31 Suppl 2:S24-28.
18. Hooper DC, Jacoby GA. Topoisomerase inhibitors: fluoroquinolone mechanisms of action and resistance. *Cold Spring Harb Perspect Med.* 2016;6(9).
19. Aranha O, Zhu L, Alhasan S, Wood DP, Jr., Kuo TH, Sarkar FH. Role of mitochondria in ciprofloxacin induced apoptosis in bladder cancer cells. *J Urol.* 2002;167(3):1288-1294.

20. Pouzaud F, Dutot M, Martin C, Debray M, Warnet JM, Rat P. Age-dependent effects on redox status, oxidative stress, mitochondrial activity and toxicity induced by fluoroquinolones on primary cultures of rabbit tendon cells. *Comp Biochem Physiol C Toxicol Pharmacol.* 2006;143(2):232-241.
21. Barnhill AE, Brewer MT, Carlson SA. Adverse effects of antimicrobials via predictable or idiosyncratic inhibition of host mitochondrial components. *Antimicrob Agents Chemother.* 2012;56(8):4046-4051.
22. Yu M, Li R, Zhang J. Repositioning of antibiotic levofloxacin as a mitochondrial biogenesis inhibitor to target breast cancer. *Biochem Biophys Res Commun.* 2016;471(4):639-645.
23. Song M, Wu H, Wu S, et al. Antibiotic drug levofloxacin inhibits proliferation and induces apoptosis of lung cancer cells through inducing mitochondrial dysfunction and oxidative damage. *Biomed Pharmacother.* 2016;84:1137-1143.
24. Wu J, Sun L, Chen X, et al. Cyclic GMP-AMP is an endogenous second messenger in innate immune signaling by cytosolic DNA. *Science.* 2013;339(6121):826-830.
25. Ablasser A, Goldeck M, Cavlar T, et al. cGAS produces a 2'-5'-linked cyclic dinucleotide second messenger that activates STING. *Nature.* 2013;498(7454):380-384.
26. Zhang X, Shi H, Wu J, Sun L, Chen C, Chen ZJ. Cyclic GMP-AMP containing mixed phosphodiester linkages is an endogenous high-affinity ligand for STING. *Mol Cell.* 2013;51(2):226-235.
27. Ouyang S, Song X, Wang Y, et al. Structural analysis of the STING adaptor protein reveals a hydrophobic dimer interface and mode of cyclic di-GMP binding. *Immunity.* 2012;36(6):1073-1086.
28. Sun L, Wu J, Du F, Chen X, Chen ZJ. Cyclic GMP-AMP synthase is a cytosolic DNA sensor that activates the type I interferon pathway. *Science.* 2013;339(6121):786-791.
29. Lee CC, Lee MT, Chen YS, et al. Risk of aortic dissection and aortic aneurysm in patients taking oral fluoroquinolone. *JAMA Intern Med.* 2015;175(11):1839-1847.
30. Daneman N, Lu H, Redelmeier DA. Fluoroquinolones and collagen associated severe adverse events: a longitudinal cohort study. *BMJ Open.* 2015;5(11):e010077.